ENSO and greenhouse warming

Wenju Cai[1,2,], Agus Santoso[3], Guojian Wang[1], Sang-Wook Yeh[4], Soon-Il An[5], Kim Cobb[6], Mat Collins[7], Eric Guilyardi[8,9], Fei-Fei Jin[10], Jong-Seong Kug[11], Matthieu Lengaigne[8], Michael J. McPhaden[12], Ken Takahashi[13], Axel Timmermann[14], Gabriel Vecchi[15], Masahiro Watanabe[16], Lixin Wu[2]

1. CSIRO Oceans and Atmosphere Flagship, Aspendale, Victoria, Australia
2. Physical Oceanography Laboratory, Qingdao Collaborative Innovation Center of Marine Science and Technology, Ocean University of China, Qingdao, China
3. Australian Research Council (ARC) Centre of Excellence for Climate System Science and Climate Change Research Centre, Level 4 Mathews Building, The University of New South Wales, Sydney 2052, Australia
4. Department of Environmental Marine Science, Hanyang University, Ansan, South Korea
5. Department of Atmospheric Sciences, Yonsei University, Seoul, South Korea
6. School of Earth & Atmospheric Sciences, Georgia Institute of Technology, 311 Ferst Drive, Atlanta, USA
7. College of Engineering Mathematics and Physical Sciences, Harrison Building, Streatham Campus, University of Exeter, Exeter, UK
8. Laboratoire d'Océanographie et du Climat: Expérimentation et Approches Numériques (LOCEAN), IRD/UPMC/CNRS/MNHN, Paris, France
9. NCAS-Climate, University of Reading, Reading, UK
10. Department of Meteorology, SOEST, University of Hawaii, Honolulu, Hawaii, USA
11. School of Environmental Science & Engineering, Pohang University of Science and technology, Pohang, South Korea
12. NOAA/Pacific Marine Environmental Laboratory, Seattle, Washington, USA
13. Instituto Geofísico del Perú, Lima, Perú
14. IPRC, Department of Oceanography, SOEST, University of Hawaii, Honolulu, Hawaii, USA
15. Geophysical Fluid Dynamics Laboratory/NOAA, Princeton, New Jersey, USA
16. Atmosphere and Ocean Research Institute, University of Tokyo, Kashiwa, Japan

Wenju Cai: wenju.cai@csiro.au
Guojian Wang: guojian.wang@csiro.au
Agus Santoso: a.santoso@unsw.edu.au
Sang-Wook Yeh: swyeh@hanyang.ac.kr
Soon-Il An: sian@yonsei.ac.kr
Kim Cobb: kcobb@eas.gatech.edu

Mat Collins: *m.collins@exeter.ac.uk*
Eric Guilyardi: *eric.guilyardi@locean-ipsl.upmc.fr*
Fei-Fei Jin: *jff@hawaii.edu*
Jong-Seong Kug: *jskug1@gmail.com*
Matthieu Lengaigne: *matthieu.lengaigne@locean-ipsl.upmc.fr*
Michael J. McPhaden: *michael.j.mcphaden@noaa.gov*
Ken Takahashi: *ken.takahashi.igp@gmail.com*
Axel Timmermann: *axel@hawaii.edu*
Gabriel Vecchi: *gabriel.a.vecchi@noaa.gov*
Masahiro Watanabe: *hiro@aori.u-tokyo.ac.jp*
Lixin Wu: *lxwu@ouc.edu.cn*

The El Niño-Southern Oscillation (ENSO) is the dominant climate phenomenon affecting extreme weather conditions worldwide. Its response to greenhouse warming has challenged scientists for decades, despite model agreement on projected mean state changes. Recent studies have provided new insights into the elusive links between ENSO and Pacific climate mean-state changes. The projected Walker circulation slow-down is expected to weaken equatorial Pacific Ocean currents, boosting the occurrences of eastward propagating warm surface anomalies that characterise observed extreme El Niño events. Accelerated equatorial Pacific warming, particularly in the east, is expected to induce eastern equatorial Pacific extreme rainfall and extreme equatorward swings of the convergence zones, both of which are features of extreme El Niño. The frequency of extreme La Niña is also expected to increase in response to more extreme El Niños, an accelerated Maritime continent warming and surface-intensified ocean warming. ENSO-related catastrophic weather events are thus likely to occur more frequently with unabated greenhouse gas emissions. However, model biases and recent observed strengthening of the Walker circulation highlight the need for further testing as new models, observations and insights become available.

Introduction. The impacts of anthropogenic climate change may be felt through changes in modes of natural climatic variability. El Niño-Southern Oscillation (ENSO) is the most important year-to-year fluctuation of the climate system on the planet[1], varying between anomalously cold (La Niña) and warm (El Niño) conditions. Underpinning occurrences of ENSO events is the positive feedback between trade wind intensity and zonal sea surface temperature (SST) contrasts, referred to as the Bjerknes feedback. The trade winds normally pile up warm surface water in the western Pacific while upwelling colder subsurface water in the east along the equator and off the west coast of South America. The resulting east-west surface temperature contrast reinforces an east-west air pressure difference across the basin that in turn drives

71 the Trades. During La Niña, the system strengthens, but during El Niño, the trade winds weaken as
72 atmospheric pressure rises in the western Pacific and falls in the eastern Pacific. The Bjerknes
73 feedback now operates in reverse, with weakened trade winds and SST warming tendencies along the
74 equator reinforcing one another. It is still not clear what sets this quasi-oscillatory behaviour, i.e.,
75 whether ENSO is self sustaining or triggered by stochastic forcing[2]. What is clear is that ocean and
76 atmosphere preconditions are required[3], as supported by the fundamental characteristics of the mean
77 tropical climate such as thermal gradients and associated circulations that balance radiative heating[4].
78 These swings in temperature are accompanied by changes in the structure of the subsurface ocean, the
79 position of atmospheric convection, and associated global teleconnection patterns, severely disrupting
80 global weather patterns[5,6,7,8,9,10], affecting ecosystems[11] and agriculture[12] worldwide.

81 During the 1982/83 and 1997/98 extreme El Niño events[6,8], surface warming anomalies propagated
82 eastward in an uncharacteristic fashion[13,14], and massive surface warm anomalies in the eastern
83 equatorial Pacific exceeding 3°C caused an equatorward shift of the Intertropical Convergence Zone
84 (ITCZ). Catastrophic floods occurred in the eastern equatorial region of Ecuador and northern Peru[6,8].
85 The South Pacific Convergence Zone (SPCZ), the largest rainband in the Southern Hemisphere,
86 shifted equatorward by up to 1000 km (an event referred to as zonal SPCZ), spurring floods and
87 droughts in south Pacific countries and shifting extreme cyclones to regions normally not affected by
88 such events[10]. Other impacts included floods in the southwest US, disappearance of marine life, and
89 decimation of the native bird population in the Galapagos Islands[15]. The development of the 1997/98
90 extreme El Niño event was accompanied by an extreme positive Indian Ocean Dipole in boreal
91 autumn, affecting millions of people across Indian Ocean-rim countries. An extreme La Niña ensued
92 in 1998/99, generating droughts in the southwest United States and eastern equatorial Pacific regions,
93 floods in the western Pacific and central American countries, and increased land-falling west Pacific
94 tropical cyclones and Atlantic hurricanes[7,9,12].

95 In light of these massive impacts, how ENSO will respond to greenhouse warming is one of the most
96 important issues in climate change science. The issue has challenged scientists for decades but there
97 has been no consensus on how ENSO amplitude and frequency may change[16,17,18]. Past studies have
98 proceeded without specifically looking into the response of ENSO extremes, and have focused on
99 simple metrics such as temperature variability in the eastern equatorial Pacific and linear dynamics,
100 assuming that the characteristics between El Niño and La Niña are symmetric. Through the Coupled
101 Model Intercomparison Phase 5 (CMIP5) process[19], substantial improvement in modelling ENSO has
102 been made[18,20,21]. There is recognition that the two opposing extremes are not a mirror
103 opposite[13,22,23,24,25,26,27]; that is, the impacts of and processes responsible for extreme El Niño and La
104 Niña events are not symmetric[14,28,29,30,31,32]. Further, the dynamics of extreme ENSO events are

105 different from moderate events[14,31,32,33], and therefore the two must be examined separately in terms of
106 their response to greenhouse warming.

107 With this recognition, significant progress has been made in understanding the characteristics of
108 extreme ENSO events in models and observations, as part of the observed diversity of events, such as
109 central Pacific ENSO[33,34,35] or ENSO Modoki[36], their likely future behaviour under greenhouse
110 conditions, and potential changes in their teleconnections. This study provides a review of these
111 advances. We show that the frequency of ENSO extremes is expected to increase, ENSO
112 teleconnections are likely to shift eastward, and these changes can, to a large extent, be interpreted as
113 consequences of mean state changes.

114 **Changes in the mean state.** The dynamics and properties of ENSO are closely linked to the slowly
115 evolving background climate state of the equatorial Pacific Ocean, for example, by rectifying into the
116 mean state[37,38], which in turn affect ENSO feedback processes[1,16]. The tropical Pacific is projected to
117 change under greenhouse warming. The projection (Box 1) includes a weakening of the Walker
118 circulation[39,40,41], a faster warming rate in the equatorial than off-equatorial Pacific[16,39,41], in the eastern
119 equatorial Pacific[41] and the Maritime continent than in the central Pacific, and over the ocean surface
120 than subsurface[32,42]. The warming pattern gives rise to an increase in rainfall in the equatorial Pacific,
121 particularly in the eastern part of the basin[43].

122 Despite a strong intermodel agreement, there is vigorous debate as to the causes of, and the
123 confidence in, these projected mean state changes. The Walker circulation is expected to weaken
124 because tropical precipitation increases at a slower rate than water vapour, so the tropical atmospheric
125 overturning must slow down with weaker equatorial Trade winds, and would occur even without a
126 change in the west-minus-east SST gradient[40]. Observations show a weakening over the past six
127 decades (1950–2009) but this was accompanied by a weakening in the west-minus-east SST gradient
128 in the Indo-Pacific[44], suggesting a coupling between oceanic and atmospheric changes. Such coupling
129 would imply that future changes of the Walker circulation need not be static or unidirectional[18,45] and
130 can be influenced, for instance, by a differential warming between the Pacific and other oceanic
131 basins. For example, a strengthening Walker circulation can be associated with a faster warming in
132 the Indian Ocean[18,46], or the Atlantic[47].

133 Another point of contention is that, in stark contrast to the projection, the Walker circulation has
134 actually strengthened over the past three decades[48,49,50,51]. The observed strengthening is suggested to
135 play a role in the so-called "global warming hiatus"[50,52], but there is debate as to its mechanism. One
136 contributing factor could be the negative phase of Interdecadal Pacific Oscillation (IPO)[50] as signified
137 by a massive western tropical Pacific sea level rise[53]. The other could be decadal variations in ENSO
138 properties, for instance, a random string of La Niña events[54], or a lack of strong eastern Pacific El

Niño events[55] but more frequent central Pacific El Niños[54] facilitated by the warmer western Pacific mean state[56]. However, the interdecadal fluctuations in ENSO properties and the IPO themselves may be inter-related, given that ENSO rectification can be a mechanism for interdecadal mean state changes[37,38].

The projected mean state changes are expected to modify ENSO's amplifying and damping feedbacks. The net change in feedbacks has been found to vary considerably across models, contributing to a lack of consensus in the change of ENSO SST variability[16,17,18]. The increased vertical temperature gradient, due to a surface-intensified ocean warming, would enhance the Ekman pumping feedback that tends to increase variability in the central Pacific[32]. The weakened easterly Trade winds would lead to an anomalous net poleward transport of warm water[16], causing the depth of the mean equatorial thermocline to shoal. This can enhance the thermocline feedback through an increased sensitivity to wind variability[18], despite being partially offset by a reduction in mean upwelling associated with the weaker mean easterly winds. Surface warming enhances evaporation and cloud cover leading to a reduction in shortwave radiation, thus increasing the efficiency of thermodynamic damping that weakens El Niño growth[16], although uncertainties remain due to models still struggling to represent the observed relationships[21]. This delicate balance between damping and amplifying feedback processes is vastly different across models[16,17,18,21]. When only models with a better representation of the various linear feedbacks are considered, an inter-model consensus in the temporal evolution of ENSO SST amplitude response is achieved[18], enhancing variability before year 2040, when SST warms faster in the eastern Pacific Ocean than over the maritime region, but decreasing variability thereafter, when the latter warms more rapidly.

The notion that ENSO properties are affected by the mean state changes appears to be supported by observations and theory[57,58]. The mid-1970 shift of the IPO from a colder to a warmer tropical eastern Pacific saw a stronger ENSO amplitude[58], marked by the 1988/1989 and 1998/99 La Niña events, which were characterised by reduced atmospheric convection in the central Pacific, and the 1982/83 and 1997/98 extreme El Niño, which featured eastward propagating SST anomalies[13,14], a shift of the ITCZ to the eastern equatorial Pacific[31], and a zonal SPCZ event[10]. Since the early 2000s, the colder eastern equatorial Pacific saw reduced ENSO SST variability in the eastern Pacific but increased SST variability in the central Pacific[25]. The asymmetric features between extreme La Niña and extreme El Niño and the vastly different changes in ENSO SST variability at different longitudes also suggest that an examination of a change in ENSO properties must move away from using only one index at a fixed location, and must take into account spatial asymmetry of ENSO anomalies.

ENSO asymmetry and extremes. El Niño and La Niña events are not symmetric in spatial pattern[22,23,24,59] or temporal evolution[13,60,61]. Extreme El Niño features disproportionately warm maximum SST anomalies in the eastern equatorial Pacific, but the anomaly centre of weak El Niño

and extreme La Niña events are situated in the central equatorial Pacific[25]. The anomaly centre of weak La Niña is located further towards the eastern equatorial Pacific than extreme La Niña[25,26,31,32]. This spatial asymmetry is characterised by positive SST skewness in the eastern equatorial Pacific, but negative skewness in the central equatorial Pacific[62]. In addition, an extreme La Niña tends to follow an extreme El Niño[27,32], but not the other way around. A La Niña can last for more than one year whereas El Niño events tend to terminate abruptly in late boreal winter or spring[13,60,61].

The asymmetries require at least two ENSO indices to distinguish extreme El Niño from extreme La Niña, or extreme El Niño from weak El Niño[25,26,31,32]. The two indices may be obtained by Empirical Orthogonal Function (EOF) analysis of SST anomalies, which deconvolves the spatio-temporal SST variability into orthogonal modes, each described by a principal spatial pattern and the corresponding principal component (PC) time series. An event may be described by an appropriately weighted superposition of the two modes. One EOF depicts strong variability in the Niño3.4 or Niño3 region[25] (Fig. 1a) and the other resembles the central Pacific El Niño pattern[34,35,36] (Fig. 1b). An extreme El Niño (**red stars,** Fig. 1c, f) is described by the difference between EOF1 and EOF2, or an E-index defined as (PC1-PC2)/$\sqrt{2}$ (Ref. 25), corresponding to extreme positive SST anomalies in the eastern equatorial Pacific (Niño3 region, Fig. 1e). An extreme La Niña (**blue stars,** Fig. 1c) is described by the sum of EOF1 and EOF2, or a large C-index defined as (PC1+PC2)/$\sqrt{2}$ (Fig. 1d) (Ref. 25), giving rise to maximum cooling in the central Pacific (Fig. 1h, i) and can be represented by SST anomalies in the Niño4 region (Fig. 1d).

Despite the recognition of inter-event differences[63], debates persist as to whether the central Pacific El Niño[34,35], whose spatial pattern resembles EOF2, is part of the ENSO asymmetry[25,26], or a distinct mode[36]. Several arguments support the view of the former. Firstly, EOF2 is a "modulator" for describing inter-event differences, and it rarely appears without a substantial projection onto EOF1. Many central Pacific El Niño events (Fig. 1g; **purple** dots in Fig. 1c, defined as when the C-index is greater than one-standard deviation) have a considerable contribution from EOF2, like La Niña events (Fig. 1d) but with an opposite sign. Even weak El Niño events (**yellow** dots Fig. 1c) involve both EOFs (Fig. 1c), and together they represent a "continuum"[33]. Indeed, warm and cold events occur over a broad range of longitudes, but their anomaly centres co-mingle[33]. Secondly, the anomaly patterns of the central Pacific El Niño and extreme La Niña are somewhat similar, and both can be represented by Niño4 (Fig. 1d). It is extreme El Niño events (**red stars**, Fig. 1c) that are outliers (Fig. 1d), exhibiting extraordinary warm anomalies inducing a massive rainfall increase in the eastern equatorial Pacific[31,64,65], without which the concept of EOF2 as an independent mode would have little basis[25].

The fact that the core of ENSO SST anomaly varies longitudinally with event magnitude reflects the asymmetry and diversity of ENSO mechanisms. Nonlinear SST-wind feedback[27,66] is thought to be a

source of ENSO asymmetry: the response of zonal winds to warm SST anomalies is greater than to cold SST anomalies. On shorter time scales, stochastic forcing including westerly wind bursts (WWBs) is more tightly coupled with warm SST anomalies than cold anomalies and the interaction between WWBs and warm SST anomalies constitutes a positive feedback[67,68]. Their coupling strengthens as the SST anomalies expand eastwards, in association with the eastward extension of the warm pool and reduced equatorial upwelling[6,8,31], contributing to larger amplitude of positive SST anomalies in the eastern equatorial Pacific[68]. For extreme El Niño, in addition to the initiation of this coupled process, as well as preconditioning by oceanic heat content[3], and enhancement by off-equatorial atmospheric conditions[30], all linear positive feedbacks (zonal advection, Ekman pumping, and thermocline feedback) play an important role in the growth of SST anomalies, and these processes strengthen as the anomaly centre moves eastward[25,69]. The zonal advective feedback process in particular is enhanced by a reversal of the equatorial currents – a feature that characterises extreme El Niño events[14,70]. At the mature phase, nonlinear vertical advection further contributes to the large positive SST anomalies[71].

The large amplitude of warm anomalies attained during an extreme El Niño induce large changes in atmospheric circulation that lead to stronger discharge of the equatorial warm water volume, abruptly terminating the event and preconditioning for a La Niña[27]. The associated thermocline shoaling in turn facilitates a more efficient Bjerknes feedback through zonal SST gradient between the Maritime region and the central Pacific[32]. Through nonlinear zonal advection (advection of anomalous zonal temperature gradient by anomalous zonal currents) and Ekman pumping, this leads to strong anomalous cooling in the central Pacific that signifies an extreme La Niña[32]. This also means that an extreme La Niña tends to develop following a strong El Niño. For central Pacific El Niño events, on the other hand, the thermocline variability and upwelling anomalies are weak due to the deep mean thermocline[33]. There, the growth of SST anomalies is largely attributed to zonal advection, though smaller in magnitude than that in the eastern Pacific[34,72,73].

Recent understanding has led to a description of extreme El Niño and extreme La Niña that is both more dynamic and impact-focused, rather than solely focussing on SST anomalies at fixed locations. An extreme El Niño event features a reversal of the upper equatorial currents to flow eastward, facilitating an eastward propagation of SST anomalies[14], a feature that is not seen during La Niña and weak El Niño events. During extreme El Niño events, the maximum total temperature is situated in the eastern equatorial Pacific. This weakens the meridional and zonal SST gradients, allowing the western Pacific convergence zone and the ITCZ to move to the eastern equatorial Pacific, an essential characteristic of an extreme El Niño event[64]. This massive reorganization of the atmospheric circulation leads to a dramatic rainfall increase in the eastern Pacific[6,8,31]. The collapse of the mean meridional SST gradients also leads to the SPCZ swinging up to 1000 km toward the equator[10]. The

use of atmospheric parameters, such as rainfall anomalies in the eastern equatorial Pacific, or outgoing longwave radiation[65] to define an El Niño[32,64], for instance, have direct ties to both local and remote impacts; it has been proven to be of great utility for examining the extreme rainfall response of El Niño to greenhouse warming[31], as underpinned by the non-linearity of atmospheric response to ENSO SSTs.

Projected changes in extreme ENSO events. Despite lingering uncertainties, the future mean state changes are robustly produced by climate models. Although most models underestimate ENSO asymmetry[59], a subset of models can simulate asymmetric and nonlinear behaviour, such as large precipitation increases over the eastern equatorial Pacific, zonal SPCZ, and eastward propagation of warm SST anomalies that characterise the observed extreme El Niño, and strong SST cooling over central Pacific associated with an extreme La Niña. As discussed further below, there is a robust projected increase in the frequency of such events and that this can be explained as consequences of the mean state changes[10,14,31,32].

However, inter-model consensus continues to be weak in terms of changes in Niño3 SST anomalies. Out of 21 models that are able to produce extreme El Niño and extreme La Niña[32], only 12 models produce an increase in ENSO amplitude (Fig. 2a). In association, only 12 models generate an increased frequency of extreme El Niño events defined as Niño3 SST greater than a 1.75-standard deviation (s.d.) value. This is despite a tendency for more occurrences of extreme cold and warm anomalies (Fig. 2c). Using the 9 models that are able to simulate the relative importance of ENSO linear feedbacks[18] does not improve the consensus. The inter-model consensus is slightly better for the Niño4 SST anomalies: 15 out the 21 (71%) models generate an increased amplitude (Fig. 2b), and 17 models produce an increased frequency in extreme La Niña, defined as when Niño4 SST is greater than a 1.75-s.d. value in amplitude, and similarly there is a tendency for more extreme cold and warm anomalies (Fig. 2d). The dynamics for the stronger consensus in Niño4 is not fully understood.

Given that extreme El Niño is characterized by a shift of the atmospheric convection to the eastern equatorial Pacific, a rainfall-based definition, e.g., as when Niño3 rainfall averaged over DJF exceeds 5 mm day^{-1}, provides an alternative avenue for assessing the frequency of such extreme events[31]. Unless stated otherwise, this rainfall-based definition of extreme El Niño is used hereafter.

Climate models suggest that the relationship between changes in mean rainfall and ENSO amplitude is complex and maybe time-varying. An increase in the eastern equatorial Pacific mean rainfall from the pre-industrial to the present-day was found to be a good indicator of increased ENSO amplitude over the same period, but for reasons still unknown, such a linkage was found not to hold for changes from the present-day to the later 21st century[43]. On the other hand, background warming tends to increase the response of rainfall to SST anomalies because rainfall responds nonlinearly to the total

temperature[74,75]. As such, there is a strong inter-model consensus on the increased rainfall response to ENSO SST anomalies, even though there is a far weaker agreement on changes in ENSO SST anomalies[75]. The increased rainfall response to ENSO anomalies is not longitudinally uniform but has a maximum that shifts increasingly eastwards with stronger ENSO SST anomalies, associated with a faster background warming in the eastern than in the central equatorial Pacific[10,74].

Mean meridional and zonal SST gradients in the equatorial Pacific are barriers to movement of convection centres, and the enhanced warming in the eastern Pacific and equatorial regions weaken these barriers. The weakening mean SST gradients make it easier for a given positive SST anomaly to further weaken or even reverse the meridional (Fig. 3a, b) and zonal SST gradients, leading to increased occurrences of strong convection and high rainfall in the eastern equatorial Pacific[31,64] (Box 1, features A and D), in spite of a convective threshold that is projected to increase with mean SSTs[76]. Consequently, the frequency of extreme El Niño increases by more than double, with a strong inter-model consensus. An analogous situation exists in the Indian Ocean, where anomalous conditions referred to as the positive Indian Ocean Dipole occurs, which features a shift of atmospheric convection to the west Indian Ocean. As a result of the weakening Walker circulation, the west tropical Indian Ocean warms faster than the east. This leads to an increase in the frequency of extreme positive Indian Ocean Dipole events[77].

The projected weakening of westward mean equatorial Pacific upper ocean currents[40,78] leads to a doubling in El Niño events that feature prominent eastward propagation of SST anomalies[14] (Box 1, feature A). Heat budget analysis shows that advection of temperature by the total current that is eastward contributes to eastward propagation of El Niño temperature anomalies[14]. Under global warming, the weakened mean current, associated with the weakened Walker circulation[40,78], favours occurrences of an eastward propagation, because it takes a smaller eastward anomaly during an El Niño to reverse the weaker westward mean current, leading to a doubling of eastward propagation events[14]. However, unlike observed extreme El Niño events, not all modelled extreme El Niño events, identified using either rainfall-based or SST-based definition, correspond with eastward propagating SST anomalies.

The projected faster warming in the equatorial than the off-equatorial Pacific[39,41,53] is expected to facilitate an increased frequency in zonal SPCZ events[10] (Box 1, feature D). In the central and western equatorial Pacific, the warmest water of the warm pool is situated south of the equator. This positive off-equatorial-minus-equatorial temperature gradient supports the southeastward extension of the SPCZ[10]. Because it is the meridional temperature gradient that is important, zonal SPCZ events can occur without an extreme El Niño[31]. The projected warming pattern results in increased occurrences of diminishing meridional SST gradients, leading to an increased frequency of zonal SPCZ events.

312 In fact, the mean state changes concurrently favour an increased frequency of extreme El Niño, zonal
313 SPCZ, and eastward propagating El Niño events, even though the dynamics for the increased
314 frequency in each type of climate extreme are not necessarily to be exactly the same. As such, the
315 frequency of any pairs of the three types of event more than doubles. Importantly, climate events
316 similar to the 1982/83 and 1997/98 events, i.e., with extreme rainfall anomalies in the eastern Pacific
317 accompanied by a zonal SPCZ and eastward propagating SST anomalies, are projected to double (Fig.
318 3a, b).

319 The projected increase in extreme El Niño events more frequently creates a favourable condition for
320 extreme La Niña events to occur, the frequency of which is expected to nearly double. The equatorial
321 Pacific thermocline tends to shoal following an El Niño, facilitating a La Niña to develop[3]. This also
322 allows more efficient Bjerknes feedback through Ekman pumping and nonlinear zonal advection –
323 processes that are important for extreme La Niña[32]. Under greenhouse warming, such favourable
324 condition is further facilitated by mean state changes (Box 1, features A and B): the increased vertical
325 temperature gradient is conducive to anomalous Ekman pumping. Faster warming over the Maritime
326 continent than in the central equatorial Pacific leads to more frequent occurrences of strong positive
327 west-minus-east temperature gradients, anomalous easterlies, anomalous oceanic westward flow and
328 upwelling, and therefore strong nonlinear zonal advection and Ekman pumping[32]. As a result,
329 aggregated over models that are able to produce extreme El Niño and La Niña[32], 75% of the increase
330 in extreme La Niña occurs after an extreme El Niño event (defined using rainfall)[32]. Approximately
331 80% of these extreme El Niño events actually correspond with Niño3 SST anomalies exceeding an
332 extreme threshold (1.75 s.d), so some 60% of the increase occurs following an SST-defined extreme
333 El Niño, analogous to the observed 1997-1998 situation. The rest of the 15% occurs following an
334 SST-defined moderate El Niño, like in 1988-89.

335 The projected increase in the frequency of extreme ENSO events is largely independent from a
336 projected increased frequency of extreme positive Indian Ocean Dipole events[77], but the sequence of
337 climate extremes similar to what the world experienced during 1997-1999, are projected to increase
338 markedly, from one in 187 years to one in 48 years (Fig. 3c, d); during these two years, an extreme
339 positive Indian Ocean Dipole preceded an extreme El Niño, and was then followed by an extreme La
340 Niña.

341 **ENSO teleconnection under greenhouse warming.** ENSO teleconnections refers to the statistically
342 significant ENSO-coherent fluctuations of a field remote from the central-to-eastern equatorial Pacific.
343 In the tropical Pacific, atmospheric teleconnections are generated through a reorganization of
344 atmospheric convection associated with ENSO SST anomalies that induce a deep baroclinic
345 response[79]. The effect is confined to the near-tropical portions of eastern Australia and western Pacific
346 countries, leading to dry conditions in these regions but wet conditions in the eastern Pacific, during

347 an El Niño. Outside the tropics, the same convective and diabatic atmospheric heating anomalies
348 excite equivalent barotropic Rossby wave trains that propagate into the northern and southern
349 extratropics[80]. Referred to as the Pacific North American pattern[81] and Pacific South American
350 pattern[82], respectively, these wave trains are the main agents for extratropical teleconnections. They
351 generate changes to midlatitude westerlies thereby affecting rainfall through changes in mean-state
352 baroclinicity, steering of storms by the westerly jet streams, and possible orographic effects[83]. There is
353 so far no study suggesting that the way in which ENSO teleconnections operate will undergo
354 fundamental changes.

355 The nonlinearity of ENSO teleconnections should continue to operate with progressing greenhouse
356 warming. Stemming from the strong asymmetry in the spatial anomaly pattern between El Niño and
357 La Niña[25,26,84,85] and between strong and moderate El Niño events[22,24,25,26,29,66], ENSO teleconnections
358 are asymmetric with respect to extreme La Niña and extreme El Niño[31,32], and with respect to weak
359 and strong events[22,36,86]. This is underpinned by several features of tropical convection. Firstly,
360 atmospheric convection tends to occur where there are maximum SSTs exceeding the convective
361 threshold (between 26^{o}C and 28^{o}C for the present-day climate)[76], so that an additional SST
362 perturbation can generate convective available potential energy as to increase the sensitivity of rainfall
363 to SST perturbations. Secondly, during an extreme El Niño event, the atmospheric convection centre
364 is displaced to the eastern equatorial Pacific[31], in contrast to an extreme La Niña, for which
365 convection, although suppressed in the central Pacific, is enhanced near its climatological position in
366 the western Pacific[32]. Thus, in terms of the convective anomaly pattern, and therefore far-field
367 teleconnections, the asymmetry between extreme La Niña and extreme El Niño is far greater than that
368 for tropical SST anomalies. A similar asymmetry is seen between a central Pacific El Niño and an
369 extreme eastern Pacific El Niño with the centre of enhanced convection located in the central
370 equatorial Pacific for the central Pacific El Niño, but in the eastern equatorial Pacific for extreme El
371 Niño[31,36]. These asymmetric features are expected to persist in a warming climate.

372 Under greenhouse warming, the response of the tropical eastern Pacific rainfall anomalies, referenced
373 to the changing mean state, to El Niño SST anomalies is likely to strengthen (Fig. 4), and the centre of
374 maximum response to shift eastward[31,75,87]. This is because rainfall responds nonlinearly to the
375 absolute SST[74,75], increasing faster in the eastern than in the western Pacific. Outside the tropics, the
376 Pacific North American pattern and the Aleutian low are expected to shift eastward, but there are
377 reported variations on how the overall intensity of this teleconnection pattern may change[87,88,89,90],
378 perhaps in part linked to a lack of consensus on how ENSO SST amplitude will change.

379 Aggregated over models that are able to produce extreme El Niño and La Niña[32], a stronger sensitivity
380 of rainfall to positive Niño3 SST anomalies (Niño3 >0.5 s.d.) in the future climate is seen in the
381 eastern equatorial Pacific and some of the extratropical oceans (left column, Fig. 4), such that even if

the amplitude of Niño3 SST variability does not change, the teleconnection has a tendency to increase in these regions. The response of rainfall to negative Niño4 SST anomalies (|Niño4| >0.5 s.d.) shows, by and large, no significant change in either the tropics or the extratropics (right column, Fig. 4), therefore the teleconnection will increase with the increased amplitude of Niño4 SST variability, which enjoys a stronger intermodel agreement. As such, future extreme El Niño and La Niña events will occur more frequently[31,32], with at least a similar strength of teleconnection to that of the present-day events. The increased frequency of ENSO extremes is consistent with an increase in ENSO-related hydroclimate variability in the tropical Pacific region, particularly in regions such as southern Asia, with important implications because these regions are already severely stressed by variations in droughts, floods and crop yields[91].

Summary, uncertainties and future research. The mean climate of the tropical Pacific is expected to change in the coming century as a result of ongoing emissions of greenhouse gases. Potential consequences of these mean state changes include more eastward propagating El Niño events, an increased frequency of extreme El Niño events as defined using extreme rainfall in the eastern equatorial Pacific, a higher frequency of extreme La Niña events, an eastward shift of the ENSO rainfall teleconnection with a likely increased intensity, and more frequent extreme equatorward swings of large-scale convergence zones, such as the SPCZ and the ITCZ. Long records of paleo-ENSO variance suggest that 20th century ENSO activity is significantly stronger than that during previous centuries[92,93] or millennia[94]. Since such paleo-records typically document changes in both ENSO-related SST and rainfall anomalies, to varying degrees, the recent intensification of ENSO in these reconstructions provides some empirical support for the projections of more extreme ENSO events under greenhouse warming.

However, there are known uncertainties that keep the confidence in these projections at the *medium* level, following the IPCC definition. The projected weakening of the Trade winds has been challenged by the observed strengthening over recent decades[48,49,51], although low frequency variability can alter long-term trends and the recent strengthening is likely associated with a negative IPO phase linked to the global warming hiatus[50,52]. The projected increased frequency of extreme El Niño and extreme La Niña events is contingent upon the faster warming in the eastern equatorial Pacific Ocean. This is in turn a balance between an ocean dynamical 'thermostat' mechanism that moderates eastern Pacific warming[95], and various other processes that enhance the warming such as a reduced poleward heat transport away[16], and surface latent heat flux adjustment and the evolution of cloud feedbacks[41]. Despite some observational support of the expected enhanced equatorial eastern Pacific warming over the past 60 years, the tropical SST trend over the recent decades has actually featured suppressed warming in the east, contrary to the expected pattern from climate models.

The ability of climate models to realistically simulate the present-day mean state climate, ENSO properties, and the associated teleconnection is another source of uncertainties. Firstly, the common "cold tongue"[96] and the double-ITCZ bias[97] in the mean state have persisted for decades, and every model suffers from its own intrinsic biases. Although in some cases models with a bias reduction produce an even higher frequency[31,32], the extent to which these biases are a source of uncertainty is yet to be tested. Secondly, we still know little about how other important characteristics of ENSO will respond to greenhouse warming, such as interactions between ENSO and the annual cycle, termination and onset of El Niño events, coupling between WWBs and El Niño, and ENSO precursors and amplifying or damping mechanisms. Thirdly, parameterisation of sub-grid physics such as atmospheric convection, cloud formation and their coupling to the resolved dynamics remains inaccurate[98]. Fourthly, the genesis and evolution of ENSO can be affected by processes occurring in the Indian and Atlantic Oceans[99,100], but the associated processes are not well understood. An additional uncertainty is whether teleconnection patterns and intensity are correctly represented at regional scales, given that the regional impacts from ENSO extremes might not be resolved by present climate models.

Before a significant reduction in these uncertainties is achieved, every effort must be made toward a projection that is consistent with our physical theoretical understanding and with what observations show. To this end, sustained ocean and atmospheric observations and effort to reduce errors are required to help determine the long-term mean state changes and to validate ENSO simulations; efforts to reduce model mean state biases, such as the "cold tongue" bias, must be bolstered; and focused observational and modelling process studies for a fuller understanding of tropical convection and cloud physics toward better parameterization for an improved ENSO simulation, must be strengthened. Although the biases and deficiencies may impede realistic simulation of ENSO extremes of the present-day and future climate, the likelihood of more frequent devastating ENSO extremes has a dynamical basis and should be considered as we prepare to face the consequences of greenhouse warming.

References

1. McPhaden, M. J., Zebiak, S. E. & Glantz, M. H. ENSO as an integrating concept in Earth science. *Science **314***, 1740-1745(2006).
2. Neelin, J. D. *et al.* ENSO theory. *J. Geophys. Res.* **103**, 14,261 (1998).
3. Jin, F.-F. An equatorial ocean recharge paradigm for ENSO. Part I: Conceptual Model. *J. Atmos. Sci.* **54**, 811-829 (1997).
4. Sun, D.-Z., El Niño: a coupled response to radiative heating? *Geophys. Res. Lett.*, **24**, 2031-2034 (1997).

5. Ropelewski, C. F. & Halpert, M. S. Global and regional scale precipitation patterns associated with the El Niño/Southern Oscillation. *Mon. Wea. Rev.* **115**, 1606–1626 (1987).
6. Philander, S. G. H. Anomalous El Niño of 1982–83. *Nature* **305**, 16 (1983).
7. Bove, M. C., O'Brien, J. J., Eisner, J. B., Landsea, C. W. & Niu, X. Effect of El Niño on US landfalling hurricanes, revisited. *Bull. Amer. Meteor. Soc.* **79**, 2477–2482 (1998).
8. McPhaden, M. J. El Niño: The child prodigy of 1997–98. *Nature* **398**, 559–562. doi:10.1038/19193 (1999).
9. Wu, M. C., Chang, W. L. & Leung, W. M. Impact of El Niño-Southern Oscillation Events on tropical cyclone landfalling activities in the western North Pacific. *J. Climate* **17**, 1419–1428 (2004).
10. Cai, W., *et al*. More extreme swings of the South Pacific convergence zone due to greenhouse warming. *Nature* **488**, 365–369 (2012).
11. Glynn, P. W. & de Weerdt, W. H. Elimination of two reef-building hydrocorals following the 1982–83 El Niño. *Science* **253**, 69–71 (1991).
12. Bell, G. D., *et al*. Climate Assessment for 1998. *Bull. Amer. Meteor. Soc.* **80**, 1040–1040 (1999).
13. McPhaden, M. J. & Zhang, X. Asymmetry in zonal phase propagation of ENSO sea surface temperature anomalies. *Geophys. Res. Lett.* **36**, L13703, doi:10.1029/2009GL038774 (2009).
14. Santoso, A., *et al*. Late-twentieth-century emergence of the El Niño propagation asymmetry and future projections. *Nature* **504**, 126–130. doi:10.1038/nature12683 (2013).
15. Valle C. A., *et al.* The Impact of the 1982–1983 E1 Niño-Southern Oscillation on Seabirds in the Galapagos Islands, Ecuador. *J. Geophys. Res*. **92**, 14,437–14,444 (1987).
16. Collins, M., *et al*. The impact of global warming on the tropical Pacific Ocean and El Niño. *Nature Geoscience* **3**, 391–397 (2010).
17. DiNezio, P. N., *et al*. Mean Climate Controls on the Simulated Response of ENSO to Increasing Greenhouse Gases. *J. Climate* **25**, 7399-7420 (2012).
18. Kim, S.-T., *et al*. Response of El Niño sea surface temperature variability to greenhouse warming. *Nature Climate Change* **4**, 786-790 (2014)
19. Taylor, K. E., Stouffer, R. J. & Meehl, G. A. An overview of CMIP5 and the experiment design. *Bull. Amer. Meteor. Soc.* **93**, 485–498 (2012).
20. Kug, J.-S., Ham, Y.-G., Lee, J.-Y. & Jin, F.-F. Improved simulation of two types of El Niño in CMIP5 models. *Environmental Research Letters* **7**, 034002 (2012).
21. Bellenger, H., *et al.* ENSO representation in climate models: from CMIP3 to CMIP5. *Clim. Dyn.* **42**, 1999-2018 (2014).
22. Hoerling, M. P., Kumar, A. & Zhong, M. El Niño, La Niña, and the nonlinearity of their teleconnections. *J. Climate* **10**, 1769–1786 (1997).
23. Rodgers, K. B., Friederichs, P. & Latif, M. Tropical pacific decadal variability and its relation to decadal modulations of ENSO. *J. Climate* **17**, 3761–3774 (2004).

24. Yu, J.-Y. & Kim, S. T. Reversed spatial asymmetries between El Niño and La Niña and their linkage to decadal ENSO modulation in CMIP3 models. *J. Climate* **24**, 5423–5434, doi:10.1175/JCLI-D-11-00024.1. (2011).
25. Takahashi, K., Montecinos, A., Goubanova, K. & Dewitte, B. ENSO regimes: Reinterpreting the canonical and Modoki El Niño. *Geophys. Res. Lett.* **38**, L10704 (2011).
Proposes that the first two empirical orthogonal function modes of tropical Pacific sea surface temperature anomalies do not describe different phenomena (i.e., El Niño-Southern Oscillation and "El Niño Modoki") but rather the nonlinear evolution of ENSO.
26. Takahashi, K. & Dewitte, B. Strong and moderate nonlinear El Niño regimes. *Climate Dyn.* DOI 10.1007/s00382-015-2665-3.(2015)
27. Choi, K.-Y., Vecchi, G. A. & Wittenberg, A. T. ENSO Transition, Duration, and Amplitude Asymmetries: Role of the Nonlinear Wind Stress Coupling in a Conceptual Model. *J. Climate* **26**, 9462–9476 (2013).
28. Timmermann, A. & Jin, F.-F. A nonlinear theory for El Niño bursting. *J. Atmos. Sci.* **60**, 152-165 (2003).
29. An, S.-I. & Jin, F.-F. Nonlinearity and asymmetry of ENSO. *J. Climate* **17**, 2399-2412 (2004).
30. Hong, L.-C., LinHo & Jin, F.-F. A Southern Hemisphere booster of super El Niño. *Geophys. Res. Lett.* **41**, 2142-2149 (2014).
Shows that preceding a super El Niño event is a transverse circulation characterized by a low-level equatorward flow, which spins off from a high sea-level-pressure anomaly around Australia and merges into the deep convection anomalies over the central Pacific, with westerly anomalies that reinforce the El Niño.
31. Cai, W., *et al*. Increasing frequency of extreme El Niño events due to greenhouse warming. *Nature Climate Change* **4,** 111–116, doi: 10.1038/nclimate2100 (2014).
32. Cai, W., *et al*. More frequent extreme La Niña events under greenhouse warming. *Nature Climate Change* **5**, 132–137, doi:10.1038/nclimate2492 (2015).
Proposes that to examine dynamics associated with extreme La Niña, Niño4 surface temperature is a more appropriate index.
33. Capotondi, A., *et al.* Understanding ENSO diversity. *Bull. Amer. Meteor. Soc.*, in press, doi:10.1175/BAMS-D-13-00117.1 (2014).
This paper uses observations, ocean reanalysis, and climate models to provide a comprehensive review of dynamics associated with different ENSO types, and to show that the basic physical processes underlying the different ENSO types are not completely distinct.
34. Kao, H. Y. & Yu, J. Y. Contrasting Eastern-Pacific and Central-Pacific Types of ENSO. *J. Climate* **22**, 615-632 (2009).
35. Yeh, S.-W., *et al*. El Niño in a changing climate. *Nature* **461**, doi: 10.1038/nature08316 (2009).

36. Ashok, K., Behera, S. K., Rao, S. A., Weng, H. & Yamagata, T. El Niño Modoki and its possible teleconnection. *J. Geophys. Res.* **112**, C11007, doi:10.1029/2006JC003798 (2007).
Suggests that El Niño Modoki, i.e., with an anomaly centre in the central equatorial Pacific, is a different type of event independent from the canonical El Niño, i.e., with an anomaly centre in the eastern equatorial Pacific.
37. Hua, L., Yu, Y. & D.-Z. Sun, D.-Z. A Further Study of ENSO Rectification: Results From an OGCM With a Seasonal Cycle. *J. Climate* **28,** 1362-1382 (2015).
Shows that the rectification effect of ENSO is to cool the western Pacific warm pool and warm the eastern equatorial Pacific.
38. Sun, D.-Z., Zhang, T., Sun, Y. & Y. Yu, Y. Rectification of El Niño-Southern Oscillation into Climate Anomalies of Decadal and Longer Time-scales: Results from Forced Ocean GCM Experiments. *J. Climate* **27**, 2545-2561 (2014).
39. Liu, Z., Vavrus, S., He, F., Wen, N. & Zhong, Y. Rethinking Tropical Ocean Response to Global Warming: The Enhanced Equatorial Warming. *J. Climate* **18**, 4684–4700 (2005).
40. Vecchi, G. A., *et al*. Weakening of tropical Pacific atmospheric circulation due to anthropogenic forcing. *Nature* **441**, 73–76 (2006).
41. Xie, S.-P., *et al.* Global warming pattern formation: sea surface temperature and rainfall. *J. Climate* **23**, 966–986 (2010).
42. An, S.-I., Kug, J.-S., Ham,Y.-G. & Kang, I.-S. Successive modulation of ENSO to the future greenhouse warming. *J.Climate* **21**, 3-21(2008).
43. Watanabe, M., *et al.* Uncertainty in the ENSO amplitude change from the past to the future. *Geophys. Res. Lett*., **39,** L20703 (2012).
44. Tokinaga, H., Xie, S.-P., Deser, C., Kosaka, Y. & Okumura, Y. M. Slowdown of the Walker circulation driven by tropical Indo-Pacific warming. *Nature* **491**, 439–443 (2012).
45. An, S.-I., *et al*. Recent and future sea surface temperature trends in tropical Pacific warm pool and cold tongue regions. *Clim. Dyn.* **39**, 1373-1383 (2012).
46. Luo, J. J., Sasaki, W. & Masumoto, Y. Indian Ocean warming modulates Pacific climate change. *Proc. Natl Acad. Sci. USA* **109**, 18701–18706 (2012).
47. McGregor, S., *et al*. Recent Walker circulation strengthening and Pacific cooling amplified by Atlantic warming. *Nature Climate Change* **4**, 888–892 (2014).
48. Solomon, A. & Newman, M. Reconciling disparate twentieth-century Indo-Pacific ocean temperature trends in the instrumental record. *Nature Climate Change* **2**, 691–699 (2012).
49. Dong, B. W. & Lu, R. Y. Interdecadal enhancement of the Walker circulation over the Tropical Pacific in the late 1990s. *Advances in Atmospheric Sciences* **30**, 247–262 (2013).
50. England, M. H., *et al.* Recently intensified Pacific Ocean wind-driven circulation and the ongoing warming hiatus. *Nature Climate Change* **4**, 222-227 (2014).

51. L'Heureux, M., Lee, S. & Lyon, B. Recent multidecadal strengthening of the Walker circulation across the tropical Pacific. *Nature Climate Change* **3**, 571–576 (2013).

52. Kosaka, Y. & Xie, S-P. Recent global-warming hiatus tied to equatorial Pacific surface cooling. *Nature* **501**, 403-407 (2013).

53. Timmermann, **A**., McGregor, S. & Jin, F.-F. Wind effects on past and future regional Sea level trends in the Southern Indo-Pacific. *J. Climate* **23**, 4429-4437(2010).

54. McPhaden, M. J., Lee, T. & McClurg, D. El Niño and its relationship to changing background conditions in the tropical Pacific Ocean. *Geophys. Res. Lett.* **38**, L15709 (2011).

55. Wittenberg, A. T., Rosati, A., Delworth, T. L., Vecchi, G. A. & Zeng, F. ENSO modulation: Is it decadally predictable? *J. Climate* **27**, 2667–2681(2014).

56. Xiang, B., Wang, B. & Li, T. A new paradigm for the predominance of standing Central Pacific warming after the late 1990s. *Clim. Dyn.* **41**, 327-340 (2013).

57. An, S.-I. & Wang, B. Interdecadal change of the structure of the ENSO mode and its impact on the ENSO frequency. *J. Climate* **13**, 2044-2055 (2000).

58. Fedorov, A. & Philander, S. G. Is El Niño changing? *Science* **288**, 1997-2002 (2000).

59. Zhang, T. & Sun, D.-Z. ENSO Asymmetry in CMIP5 models. *J. Climate* **27**, 4070-4093 (2014).
Shows that most models underestimate ENSO asymmetry, and that the underestimate primarily results from a weaker SST warm anomaly over the eastern Pacific and a westward shift of the centre of the anomaly.

60. Ohba, M. & Ueda, H. Role of nonlinear atmospheric response to SST on the asymmetric transition process of ENSO. *J. Climate* **22**,177–192 (2009).

61. Okumura, Y. M. & Deser, C. Asymmetry in the duration of El Niño and La Niña. *J Climate* **23**, 5826–5843 (2010).

62. Burgers, G. & Stephenson, D. B. The ‘‘normality’’ of El Niño. *Geophys. Res. Lett.*, **26**, 1027–1030 (1999).

63. Trenberth, K. E. & Stepaniak, D. P. Indices of El Niño evolution, *J. Climate* **14**, 1697–1701 (2001).

64. Lengaigne, M. & Vecchi, G.A. Contrasting the termination of moderate and extreme El Niño events in Coupled General Circulation Models. *Climate Dynamics*, **35,** 299-313(2010).
Proposes that a large rainfall anomaly in the eastern equatorial Pacific can be used to examine whether a model is able to generate an extreme El Niño.

65. Chiodi, A. M. & Harrison, D. E. El Niño impacts on seasonal U.S. atmospheric circulation, temperature, and precipitation anomalies: The OLR-event perspective. *J. Climate* **26**, 822–837 (2013).
Shows that since 1979 most of the U.S. seasonal weather impact of El Niño events is associated with the few events identified by the behavior of outgoing longwave radiation over the eastern equatorial Pacific, suggesting the utility of outgoing longwave radiation to define El Niño.

66. Frauen, C. & Dommenget, D. El Niño and La Niña amplitude asymmetry caused by atmospheric feedbacks. *Geophys. Res. Lett.* **37**, L18801 (2010).
67. Gebbie, G., Eisenman, I., Wittenberg, A. & Tziperman, E. Modulation of westerly wind bursts by sea surface temperature: A semistochastic feedback for ENSO. *J. Atmos. Sci*. **64**, 3281-3295 (2007).
68. Lengaigne, M., *et al.* The March 1997 Westerly Wind Event and the onset of the 1997/98 El Niño: understanding the role of the atmospheric response. *J Climate* **16**(20), 3330–3343 (2003).
69. An, S.-I. & Jin, F.-F. Collective role of thermocline and zonal advective feedbacks in the ENSO mode. *J Climate* **14**, 3421–3432 (2001).
70. Kim, W. & Cai, W. The importance of the eastward zonal current for generating extreme El Niño. *Clim. Dyn.* **42**, 3005-3014 (2014).
Finds that the eastward zonal current, seen only during extreme El Niño, plays an important role in making an El Niño event extreme.
71. Jin, F.-F., An, S.-I., Timmermann, A. & Zhao, J. Strong El Niño events and nonlinear dynamical heating. *Geophys. Res. Lett.* **30**(3), 1120 (2003).
72. Lübbecke, J. & McPhaden, M. J. Assessing the Twenty-First-Century shift in ENSO variability in terms of the Bjerknes stability index. *J. Climate* **27**, 2577-2587 (2014).
73. Newman, M., Alexander, M. A. & Scott, J. D. An empirical model of tropical ocean dynamics. *Clim. Dyn.* **37**, 1823-1841 (2011).
74. Chung, C. T. Y., Power, S. B., Arblaster, J. M., Rashid, H. A. & Roff, G. L. Nonlinear Precipitation Response to El Niño and Global Warming in the Indo-Pacific. *Clim. Dyn*. **42**, 1837-1856 (2013).
75. Power, S. B., Delage, F., Chung, C. T. Y., Kociuba, G. & Keay, K. Robust twenty-first century projections of El Niño and related precipitation variability. *Nature* **502**, 541–547 (2014).
76. Johnson, N. C. & Xie, S.-P. Changes in the sea surface temperature threshold for tropical convection. *Nature Geoscience* **3**, 842-845 (2010).
Demonstrates that under global warming, surface temperature threshold for tropical atmospheric convection increases commensurately with mean temperature over the tropics.
77. Cai, W., *et al.* Increased frequency of extreme Indian Ocean Dipole events due to greenhouse warming. *Nature* **510**, 254-258 (2014).
78. Sen Gupta, A., Ganachaud, A., McGregor, S., Brown, J. N. & Muir, L. Drivers of the projected changes to the Pacific Ocean equatorial circulation. *Geophys. Res. Lett.* L09605 (2012).
79. Gill, A. E. Some simple solutions for heat-induced tropical circulation. *Quart. J. Roy. Meteor. Soc.* **106**, 447–462 (1980).
80. Hoskins, B. J. & Karoly, D. J. The steady linear response of a spherical atmosphere to thermal and orographic forcing. *J. Atmos. Sci.* **38**, 1179–1196 (1981).

81. Horel, J. D. & Wallace, J. M. Planetary-scale atmospheric phenomena associated with the Southern Oscillation. *Mon. Wea. Rev.* **109**, 813–829 (1981).
82. Karoly, D. J. Southern Hemisphere circulation features associated with El Niño–Southern Oscillation events. *J. Climate* **2**, 1239–1252 (1989).
83. Cai, W., van Rensch, P., Cowan, T. & Hendon, H. H. Teleconnections pathways of ENSO and IOD and the mechanisms for impacts on Australian rainfall. *J. Climate* **24**, 3910 (2011).
84. Okumura, Y. M., Ohba, M., Deser, C., & Ueda, H. A proposed mechanism for the asymmetric duration of El Niño and La Niña. *J. Climate* **24**, 3822–3829 (2011).
85. DiNezio, P. N. & Deser, C. Nonlinear Controls on the Persistence of La Niña. *J. Climate* **27**, 7335–7355 (2014).
86. Zhang, W. J., Jin, F.-F., Ren, H.-L., Li, J. & Zhao, J.-X. Differences in teleconnection over the North Pacific and rainfall shift over the USA associated with two types of El Niño during boreal autumn. *J. Meteor. Soc. Japan* **90**, 535–552 (2012).
87. Kug, J.-S., An, S.-I., Ham, Y.-G. & Kang, I.-S. Changes in El Niño and La Niña teleconnections over North Pacific-America in the global warming simulations. *Theor. Appl. Climatol.* **100**, 275–282 (2010).
88. Meehl, G. A., & Teng, H. Multi-model changes in El Niño teleconnections over North America in a future warmer climate. *Clim. Dyn.* **29**, 779–790, doi:10.1007/s00382-007-0268-3 (2007).
89. Stevenson, S. L. Significant changes to ENSO strength and impacts in the twenty-first century: Results from CMIP5. *Geophy. Res. Lett.* **39**, L17703 (2012).
90. Zhou, Z.-Q., *et al.* Global warming-induced changes in El Niño teleconnections over the North Pacific and North America. *J. Climate* **27**, 9050–9064 (2014).
91. Seager, R., Naik, N., & Vogel, L. Does global warming cause intensified interannual hydroclimate variability? *J. Climate* **25**, 3355-3372 (2012).
92. McGregor, S., Timmermann, A., England, M. H., Elison Timm, O., and Wittenberg, A. T. Inferred changes in El Niño-Southern Oscillation variance over the past six centuries. *Climate of the Past* , 9, 2269-2284 (2013).
93. Li, J., *et al*. El Niño modulations over the past seven centuries, *Nature Climate Change*, **3**, 822–826 (2013).
94. Cobb, K. M. *et al.* Highly variable El Niño-Southern Oscillation throughout the Holocene. *Science* **339,** 67–70 (2013).
95. Cane, M. A., *et al*. Twentieth century sea surface temperature trends. *Science* **275**, 957-960 (1997).
96. Li, G. & Xie, S.-P. Tropical Biases in CMIP5 Multimodel Ensemble: The Excessive Equatorial Pacific Cold Tongue and Double ITCZ Problems. *J. Climate* **27**, 1765–1780 (2014).
97. Bellucci, A., Gualdi, S., Navarra, A. The double-ITCZ syndrome in coupled general circulation models: The role of large-scale vertical circulation regimes. *J. Climate* **23**, 1127-1145 (2009).

670 98. Bony, S. & Dufresne, J. L. Marine boundary layer clouds at the heart of tropical cloud feedback
671 uncertainties in climate models. *Geophys. Res. Lett.* **32**, L20806 (2005).
672 99. Izumo T., *et al*. Influence of the state of the Indian Ocean Dipole on the following year's El Niño.
673 *Nature Geoscience* **3**, 168–172 (2010).
674 100. Ham, Y. G., Kug, J. S., Park, J. Y. & Jin, F. F. Sea Surface Temperature in the North Tropical
675 Atlantic as a Trigger for El Niño/Southern Oscillation Events. *Nature Geoscience* **6**, 112-116
676 (2013).

677 **Additional information**

678 Reprints and permissions information is available at www.nature.com/nature. Correspondence and
679 requests for materials should be addressed to W.C.

680 **Acknowledgements**

681 W.C. and G.W. are supported by the Australian Climate Change Science Program and a CSIRO
682 Office of Chief Executive Science Leader award. A.S. is supported by the Australian Research
683 Council. M.C. was supported by NERC NE/I022841/1. S.W.Y. is supported by the National
684 Research Fund of Korea
685 grant funded by the Korean Government (MEST) (NRF-2009-C1AAA001-2009-0093042). S. I.
686 A. was supported by Basic Science Research Program through the National Research Foundation of
687 Korea funded by the Ministry of Science, ICT and future Planning (No. 2014R1A2A1A11049497).
688 This is PMEL contribution number ****.

689 **Author Contributions**

690 W.C., A.S. G.W., and S.W.Y wrote the initial version of the paper. G.W. performed the model output
691 analysis and generated all Figures. All authors contributed to interpreting results, discussion of the
692 associated dynamics, and improvement of this paper.

693 **Author Information** Reprints and permissions information are available at:www.nature.com/reprints.
694 The authors declare no competing financial interests. Correspondence and requests for materials
695 should be addressed to Wenju Cai (wenju.cai@csiro.au).

696

Figure captions

Figure 1 | Observed ENSO asymmetry. **a, b,** First and second principal variability patterns of SST obtained by applying EOF analysis to satellite-era SST anomalies in austral summer (DJF), in the tropical Pacific region of 15°S–15°N, 140°–280°E. The SST anomalies and wind stress vectors are presented as linear regression onto standardized principal component (PC) time series. **c,** Relationship between the two principal component time series. **d,** Relationship between C-index and Niño4 SST index (160°E–150°W, 5°S–5°N, indicated by the blue box in each panel). The C-index is defined as (PC1+PC2)/$\sqrt{2}$. **e,** Relationship between E-index and Niño3 SST index (150°W–90°W, 5°S–5°N, indicated by the red box in each panel). The E-index is defined as (PC1-PC2)/$\sqrt{2}$. **f,** **Blue stars** indicate **extreme La Niña** events, i.e., 1988/89 and 1998/99, defined as when both principal components are negative but greater than 1 s.d. in amplitude (as shown in panel **c**), or quadratically detrended Niño4 is negative but greater than 1.75 s.d. in amplitude (as shown in panel **d**); **light blue** dots indicate **moderate La Niña** events, i.e., 1983/84, 1999/00, 2007/08 and 2010/11, defined as when the negative Niño4 (unit in s.d) is greater than 1 s.d. but less than 1.75 s.d. in amplitude (as shown in panel **d**); **green** dots indicate **weak La Niña** events, i.e., 1984/85, 1995/96, 2000/01 and 2008/09, defined as when the negative Niño4 is greater than 0.5 s.d. but less than 1 s.d. in amplitude (as shown in panel **d**); **red stars** indicate **extreme El Niño** events, i.e., 1982/83 and 1997/98, defined as when EOF1 is greater than 1 s.d. and negative EOF2 is greater than 1 s.d. in amplitude (as shown in panel **c**); **purple** dots indicate **central-Pacific El Niño** events, i.e., 1990/91, 2002/03, 2004/05 and 2009/10, defined as when C-index is greater than 1 s.d. (as shown in panel **d**); **yellow** dots indicate events that are **a mixture of central-Pacific and eastern-Pacific El Niño events,** i.e., 1979/80, 1986/87, 1987/88, 1991/92, 1994/95, 2001/02, 2003/04 and 2006/07, defined as when C-index is greater than 0.5 s.d. but less than 1 s.d. (as shown in panel **d**). **f – i,** anomaly pattern of extreme El Niño, CP El Niño, extreme La Niña, and weak La Niña, respectively.

Figure 2 | Greenhouse warming-induced changes in ENSO properties. Shown are based on outputs from CMIP5 experiments under historical and RCP8.5 scenarios using 21 models (out of 34 in total), focusing on austral summer (DJF)**. a, b,** Comparison of Niño3 and Niño4 standard deviation (s.d) in the *Control* period (1900-1999) (x-axis) and *Climate change* period (2000-2099) (y-axis). Numbers in the upper left indicate the number of models that produce an increase in s.d., and in the lower right, number of models that produce a decrease in s.d. **c, d,** Histogram of quadratically detrended Niño3 and Niño4 SST anomalies in s.d. for *Control* period (1900-1999) (**blue**) and *Climate change* period (2000-2099) (**red**). There is a tendency for each index to be more extreme, but the two histograms in each panel are not statistically different (H=0) about the 95% confidence interval, using a 2-sided student-*t* test.

Figure 3 | Greenhouse warming-induced changes in climate extremes. Shown are based on outputs from CMIP5 experiments under historical and RCP8.5 scenarios using 21 models (out of 34 in total), focusing on austral summer (DJF)**.** In all panels, extreme El Niño is defined as when Niño3 rainfall is greater than 5 mm/day[31]. **a** and **b**, extreme El Niño events concurrent with eastward propagating SST anomalies[14] and zonal SPCZ events[10] (**blue stars**), similar to the 1997/98 extreme El Niño event, for the *Control* period (1900-1999) and *Climate change* period (2000-2099), respectively. The frequency of such events almost doubles. **c** and **d,** Extreme El Niño events preceded by an extreme positive Indian Ocean Dipole, and followed by an extreme La Niña (**red stars**), similar to what happened in 1997-1999, for the *Control* period (1900-1999) and *Climate change* period (2000-2099), respectively.

Figure 4 | Greenhouse warming-induced change in rainfall response to Niño3 and Niño4 SST anomalies. Shown are based on outputs from CMIP5 experiments under historical and RCP8.5 scenarios using 21 models (out of 34 in total), focusing on austral summer (DJF)**. a, b,** Multi-model average of quadratically detrended rainfall anomalies associated with El Niño, obtained by regressing quadratically detrended rainfall anomalies onto quadratically detrended Niño3 using samples with Niño3 greater than positive 0.5 s.d., in *Control* and *Climate change* periods, respectively. **c,** The difference between **a** and **b** (i.e., **b-a**). Stippling in **c** indicates regions where the difference is statistically significant above the 95% confidence level as determined by a two-sided Student's *t*-test. **d, e** and **f** are the same as **a, b** and **c**, respectively, but for the patterns associated with La Niña, using samples with a Niño4 greater than 0.5 s.d. in amplitude.

Box 1 | Mean state changes and consequences

(Insert Box Figure)

Box Figure | Schematic showing greenhouse-induced future changes at the surface (shown only for the north Pacific) and upper ocean along-equator and meridional cross-sections. **Greenhouse-induced changes** (**red** arrows) to the mean Walker circulation (**dashed black** with shadow) and **mean ocean currents** (**cyan arrows**) are indicated. Major features of changes are indicated by letters **A**, **B**, **C**, and **D**.

A Features associated with a weakening Walker circulation. The Trade winds and equatorial currents weaken, the eastern equatorial Pacific warms faster that the surrounding regions, and the thermocline shallows (**present-day: black curve**; **future: red curve**). The weakening equatorial zonal currents are conducive to an increased frequency of eastward propagating El Niño events. The faster warming in the eastern equatorial Pacific is favourable for an increased frequency of extreme El Niño events by promoting atmospheric convection. The increased occurrences of extreme El Niño are

764 in turn conducive to an increased frequency of La Niña due to a discharged thermocline that promotes
765 an influence of the subsurface cool water in the central Pacific.

766 **B Increasing vertical temperature gradients, and C enhanced warming over the maritime**
767 **continent.** These changes are additional factors that facilitate an increased frequency of extreme La
768 Niña events, through nonlinear zonal advection and Ekman pumping.

769 **D Accelerated warming in the equatorial rather than in the off-equtorial Pacific.** This change
770 leads to an increased frequency of equatorward shifts of the ITCZ, which characterizes an extreme El
771 Niño, and to an increased frequency of extreme swings of the SPCZ toward the equator. This occurs
772 because atmospheric convection tends to follow maximum sea surface temperatures.

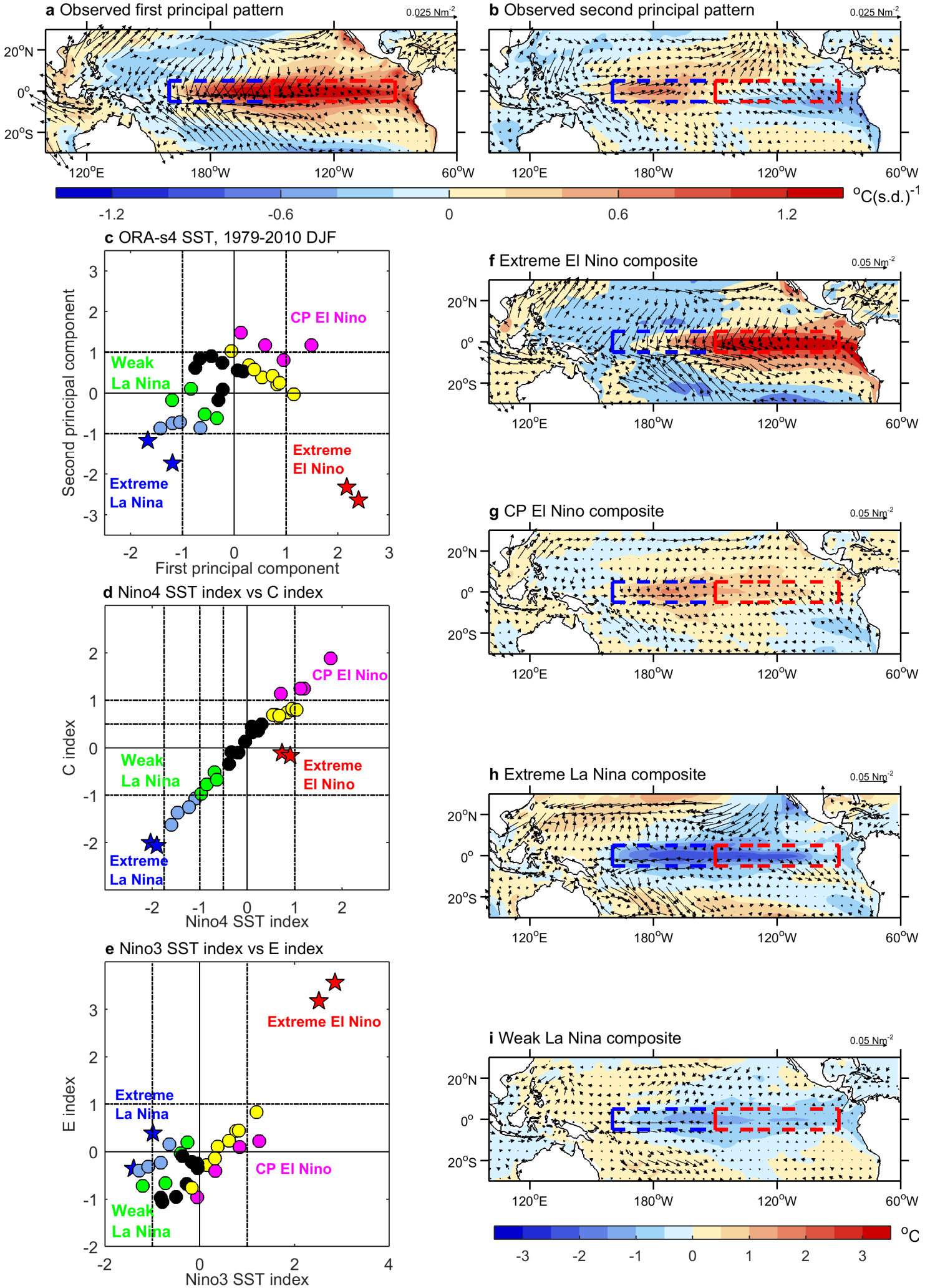
a Observed first principal pattern
0.025 Nm-2
b Observed second principal pattern
0.025 Nm-2
20°N
0°
20°S
120°E
180°W
120°W
60°W
-1.2
-0.6
0
0.6
1.2
°C(s.d.)-1
c ORA-s4 SST, 1979-2010 DJF
Second principal component
First principal component
CP El Nino
Weak La Nina
Extreme El Nino
Extreme La Nina
d Nino4 SST index vs C index
C index
Nino4 SST index
e Nino3 SST index vs E index
E index
Nino3 SST index
f Extreme El Nino composite
0.05 Nm-2
g CP El Nino composite
h Extreme La Nina composite
i Weak La Nina composite
°C

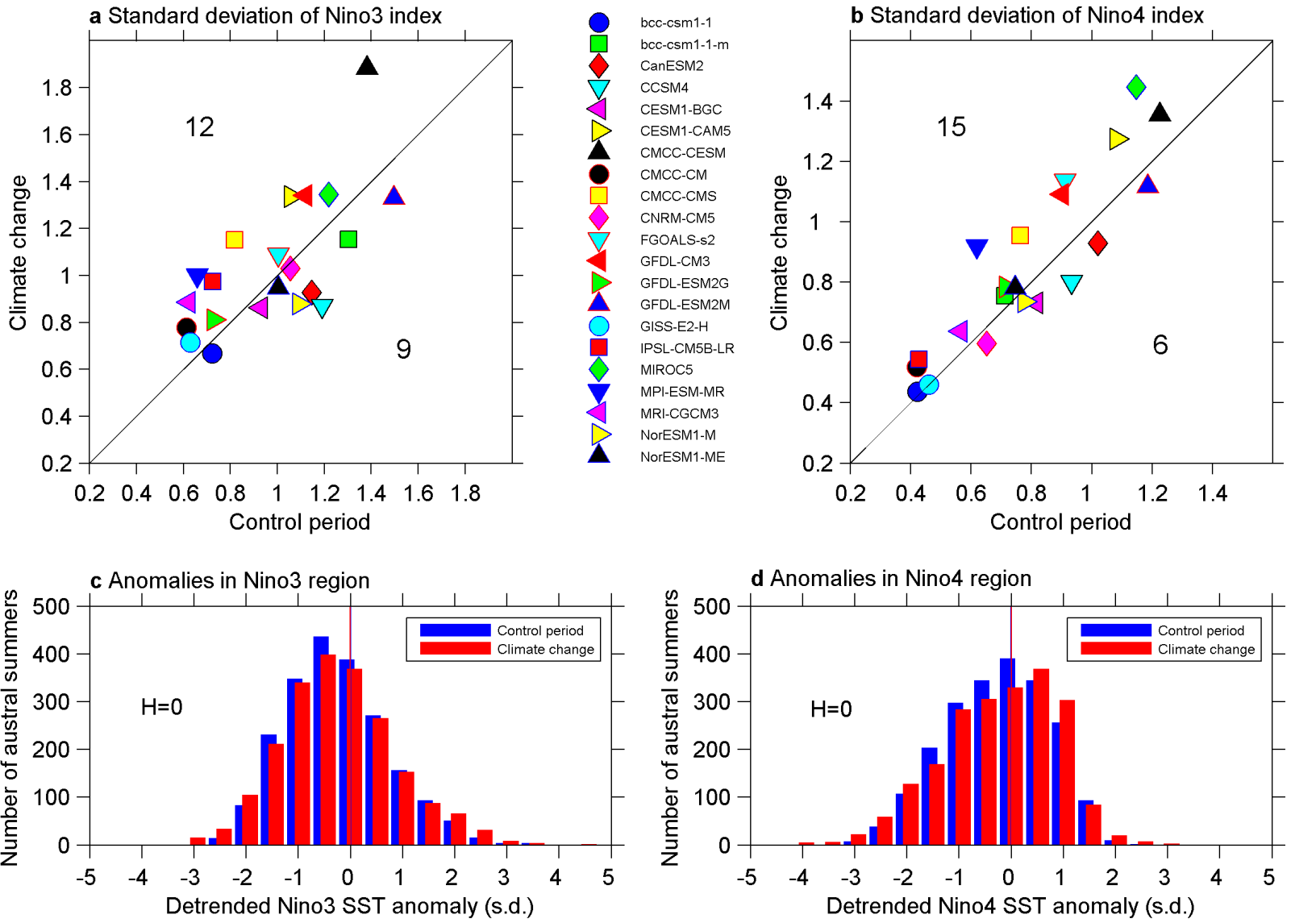
a Standard deviation of Nino3 index
Climate change
Control period
12
9
b Standard deviation of Nino4 index
15
6
bcc-csm1-1
bcc-csm1-1-m
CanESM2
CCSM4
CESM1-BGC
CESM1-CAM5
CMCC-CESM
CMCC-CM
CMCC-CMS
CNRM-CM5
FGOALS-s2
GFDL-CM3
GFDL-ESM2G
GFDL-ESM2M
GISS-E2-H
IPSL-CM5B-LR
MIROC5
MPI-ESM-MR
MRI-CGCM3
NorESM1-M
NorESM1-ME

c Anomalies in Nino3 region
Number of austral summers
Control period
Climate change
H=0
Detrended Nino3 SST anomaly (s.d.)

d Anomalies in Nino4 region
Number of austral summers
Control period
Climate change
H=0
Detrended Nino4 SST anomaly (s.d.)

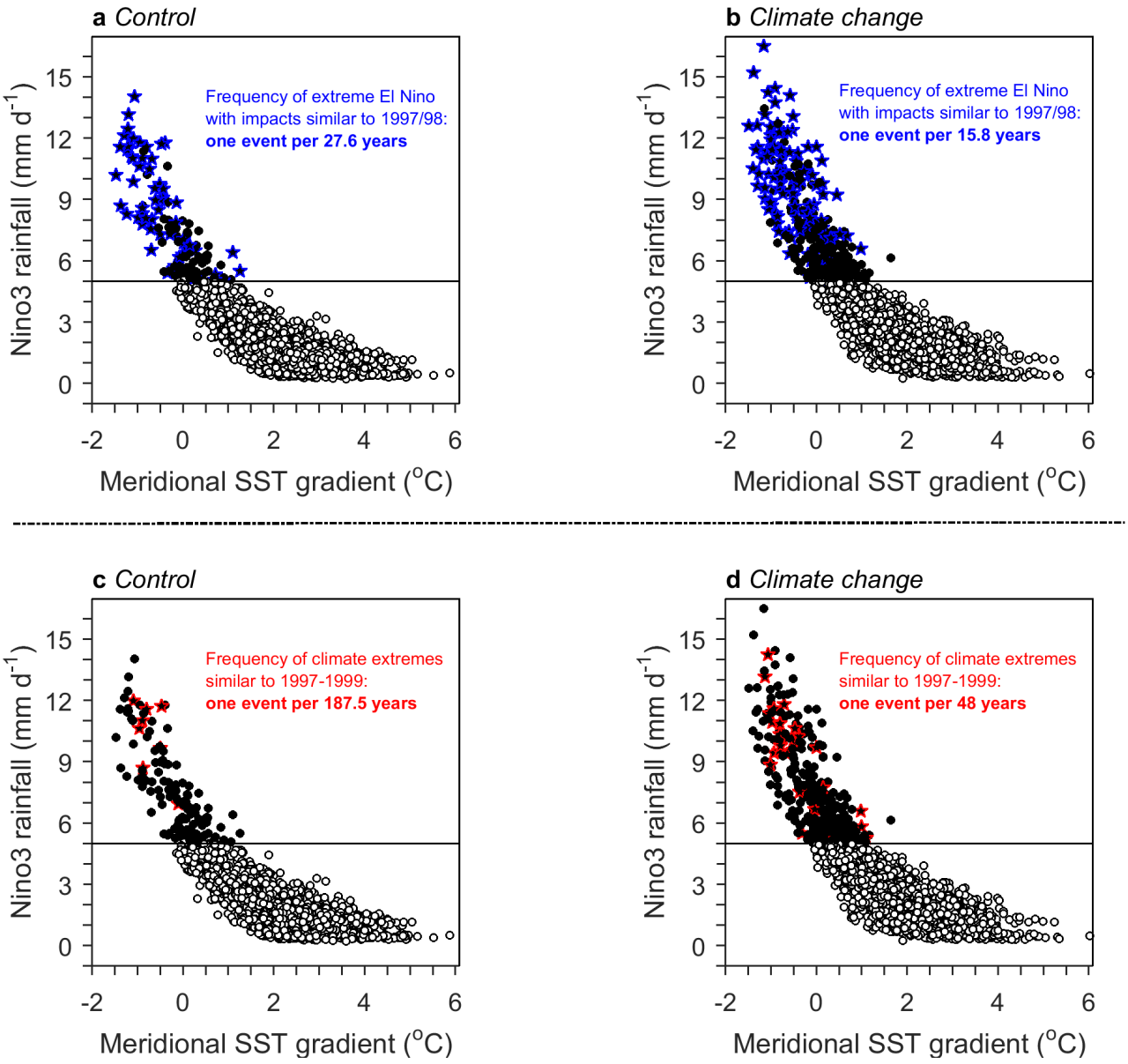
a Control
Frequency of extreme El Nino
with impacts similar to 1997/98:
one event per 27.6 years
Nino3 rainfall (mm d-1)
Meridional SST gradient (°C)
b Climate change
Frequency of extreme El Nino
with impacts similar to 1997/98:
one event per 15.8 years
Nino3 rainfall (mm d-1)
Meridional SST gradient (°C)
c Control
Frequency of climate extremes
similar to 1997-1999:
one event per 187.5 years
Nino3 rainfall (mm d-1)
Meridional SST gradient (°C)
d Climate change
Frequency of climate extremes
similar to 1997-1999:
one event per 48 years
Nino3 rainfall (mm d-1)
Meridional SST gradient (°C)

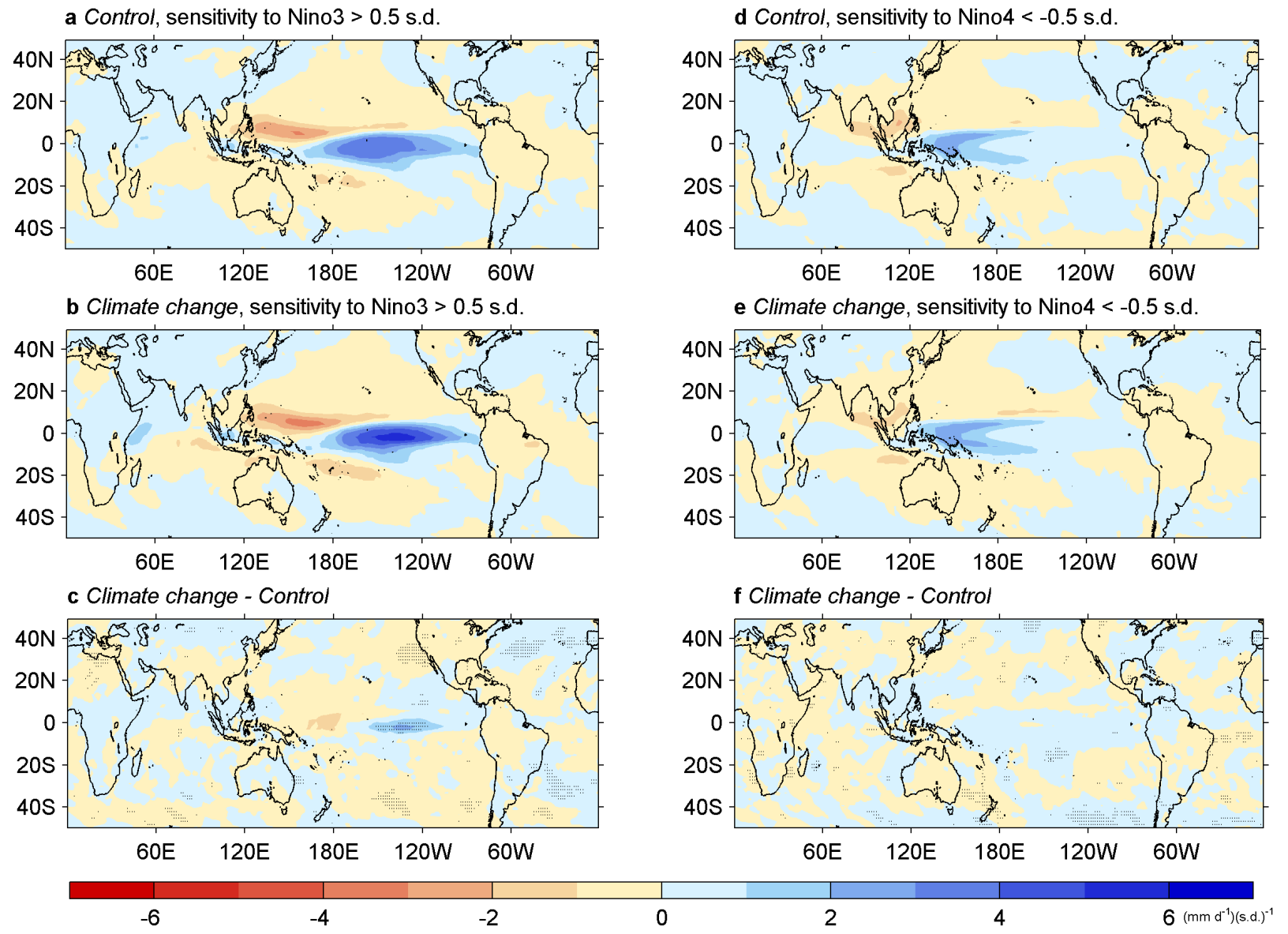
a Control, sensitivity to Nino3 > 0.5 s.d.
d Control, sensitivity to Nino4 < -0.5 s.d.
b Climate change, sensitivity to Nino3 > 0.5 s.d.
e Climate change, sensitivity to Nino4 < -0.5 s.d.
c Climate change - Control
f Climate change - Control
40N
20N
0
20S
40S
60E
120E
180E
120W
60W
-6
-4
-2
0
2
4
6
(mm d-1)(s.d.)-1

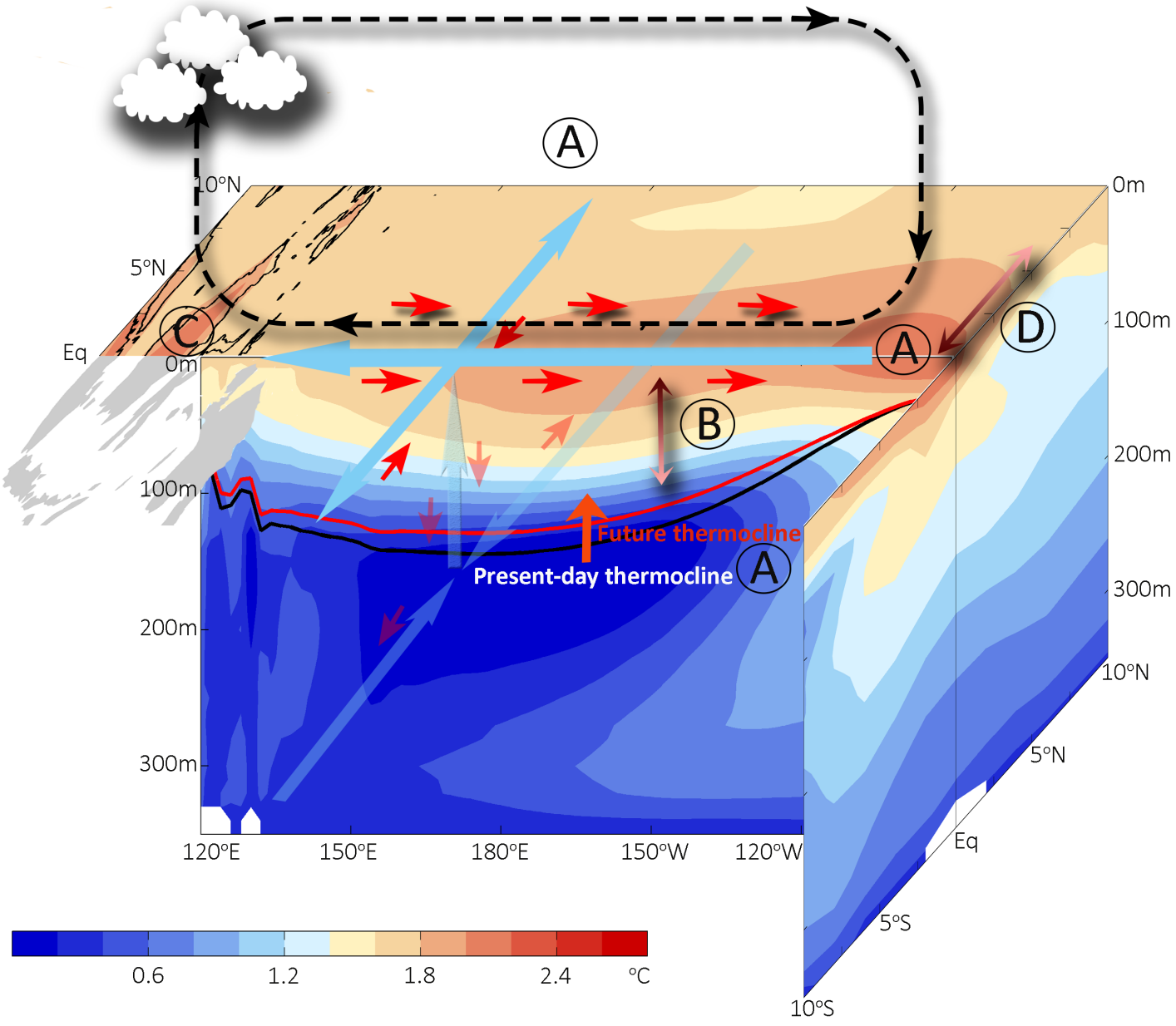
A
10°N
5°N
Eq
C
0m
A
D
B
100m
200m
300m
Future thermocline
Present-day thermocline
A
120°E
150°E
180°E
150°W
120°W
0m
100m
200m
300m
10°N
5°N
Eq
5°S
10°S
0.6
1.2
1.8
2.4
°C